

Spherical scalar waves and gravity - red shift and backscattering

Edward Malec

Jagiellonian University, Institute of Physics, 30-59 Kraków, Reymonta 4, Poland

Niall Ó Murchadha

Physics Department, University College, Cork, Ireland

Tadeusz Chmaj

Institute of Nuclear Physics, Kraków, Radzikowskiego 152, Poland

This article investigates the interaction of a spherically symmetric massless scalar field with a strong gravitational field. It focuses on the propagation of waves in regions outside any horizons. The two factors acting on the waves can be identified as a redshift and a backscattering. The influence of backscattering on the intensity of the outgoing radiation is studied and rigorous quantitative upper bounds obtained. These show that the total flux may be decreased if the sources are placed in a region adjoining an apparent horizon. Backscattering can be neglected in the case $2m_0/R \ll 1$, that is when the emitter is located at a distance from a black hole much larger than the Schwarzschild radius. This backscattering may have noticeable astrophysical consequences.

04.20.-q, 04.30.Nk, 04.40.-b, 95.30.Sf

I. INTRODUCTION.

A black hole can be investigated by observing the gravitational radiation or the electromagnetic radiation emitted by a medium surrounding it. The two major effects that act on the radiation are redshift and backscatter. While the redshift is well understood, little attention has been focused to date on backscattering, a phenomenon that prevents radiation from being transmitted exclusively along null cones. Backscattering can influence observations, since sharp and strong initial impulses can be weakened and dispersed. Electromagnetic or gravitational radiation, for instance, reaching an asymptotic observer, can be weaker than expected.

In this paper we assess analytically this effect by considering as a toy model a spherically symmetric massless scalar field. This simplifying assumption should not restrict seriously the validity of our conclusions. We study the evolution of pulses of radiation which are initially purely outgoing and emitted from a region close to a spherical black hole. Rigorous upper bounds on the magnitude of the backscattering effect are obtained; these estimates, while they break down close to the horizon, allow one to recognise the regions in which the backscattering may be neglected. We estimate how significant this effect would be in the case of neutron stars or black holes. The analytic estimates that are obtained here can be used in numerical gravity in order to assess numerical codes. They can be used to test both the accuracy and the long-time stability of the numerical models. The final section outlines possible astrophysical consequences of backscattering.

Our results give the first, we believe, quantitative measure of this strong field effect. It is worthwhile pointing out that both our approach and the physical problem dealt with are different from that discussed in the existing literature on backscattering, which concentrates on the analysis of stationary radiation on a fixed geometric background [1].

II. SPHERICALLY SYMMETRIC MASSLESS SCALAR FIELDS IN MINKOWSKI SPACE

Let us consider Minkowski space with a spherically symmetric coordinate system and a metric $g_{\mu\nu} = (-1, +1, R^2, R^2 \sin^2 \theta)$. Let $\phi(R, t)$ be a spherical field which satisfies the simplest massless wave equation

$$\nabla^\mu \nabla_\mu \phi = 0. \quad (2.1)$$

The general solution (except at the origin) to Eq.(2.1) is

$$\phi = \frac{f(R+t) + g(R-t)}{R}, \quad (2.2)$$

where f and g are essentially arbitrary functions of one variable. Therefore the general solution can be regarded as a superposition of an ingoing null field f and an outgoing null field g . Associated with the field ϕ will be a stress-energy

tensor $T_{\mu\nu}$, an object of some importance, as we want to couple the scalar field to gravity.' *A priori*, it is required only that $T_{\mu\nu}$ be a symmetric tensor that satisfies the conservation equation $T_{\nu;\mu}^{\mu} = 0$. The standard choice is

$$T_{\mu\nu} = \nabla_{\mu}\phi\nabla_{\nu}\phi - \frac{1}{2}g_{\mu\nu}(\nabla\phi)^2. \quad (2.3)$$

This tensor will be subsequently used, but the reader should be aware that it is not necessarily unique.

Given the way that the field runs along the ingoing and outgoing null directions, it is natural to consider the two ingoing and outgoing null derivatives of ϕ

$$U = (\partial_R + \partial_t)\phi = \frac{2f'}{R} - \frac{\phi}{R} \quad (2.4)$$

$$V = (\partial_R - \partial_t)\phi = \frac{2g'}{R} - \frac{\phi}{R}. \quad (2.5)$$

When written in terms of U and V , the stress-energy tensor take a form

$$T_{00} = \frac{1}{4}(U^2 + V^2) = \rho \quad (2.6)$$

$$T_{0R} = \frac{1}{4}(U^2 - V^2) = -J \quad (2.7)$$

$$T_{RR} = \frac{1}{4}(U^2 + V^2) \quad (2.8)$$

$$T_{\theta\theta} = -\frac{1}{2}R^2UV \quad (2.9)$$

$$T_{\phi\phi} = -\frac{1}{2}R^2\sin^2\theta UV. \quad (2.10)$$

From Eqs.(2.6) and (2.7) one can be tempted to interpret V^2 and U^2 as, respectively, outgoing and ingoing components of a radial flux. There is, however, a discrepancy with what can be inferred from (. 2.2); from that follows, for instance, that field is purely outgoing if $f \equiv 0$. When returning to Eqs.(2.4) and (2.5), it is clear that then U does not vanish identically. As a consequence, if the field is purely outgoing, the energy-momentum has an inward part which only vanishes asymptotically so that the energy-momentum is timelike even though the field is null.

There do exist objects which more naturally reflect the splitting given by Eq.(2.2) into ingoing and outgoing modes. Let us define

$$h_+(R, t) = \frac{1}{2}(\partial_R - \partial_t)(R\phi) = g' = \frac{RV}{2} + \frac{\phi}{2} \quad (2.11)$$

$$h_-(R, t) = \frac{1}{2}(\partial_R + \partial_t)(R\phi) = f' = \frac{RU}{2} + \frac{\phi}{2}. \quad (2.12)$$

Extending R to cover the whole real line and defining $h(R, t)$ via

$$h(R, t) = h_+(R, t), R > 0 \quad (2.13)$$

$$h(R, t) = h_-(R, t), R \leq 0, \quad (2.14)$$

allows one to write the field equation (2.1) compactly as

$$(\partial_R + \partial_t)h(R, t) = 0. \quad (2.15)$$

By comparison, when writing earlier the field equation in terms of U and V we get a pair of coupled equations. There exists another stress-energy tensor, more naturally related to h_{\pm} , of the form

$$T'_{00} = \frac{h_+^2 + h_-^2}{R^2} \quad (2.16)$$

$$T'_{0R} = \frac{h_-^2 - h_+^2}{R^2} \quad (2.17)$$

$$T'_{RR} = T'_{00} \quad (2.18)$$

$$T'_{\theta\theta} = T'_{\phi\phi} = 0. \quad (2.19)$$

This also satisfies $T'_{\nu;\mu}^{\mu} = 0$ in flat space. Unfortunately, it is not clear how to generalize that object to curved space so we will restrict our attention to the $T^{\mu\nu}$ as defined by Eqs.(2.6 - 2.10). While the field equation is best expressed in terms of $h(R, t)$, as will be shown later, the conserved quantities are natural in terms of U and V .

The total energy inside a sphere of radius R at a fixed time t reads

$$M(R, t) = 4\pi \int_0^R r^2 \rho dr = 4\pi \int_0^R r^2 T_{00} dr = \pi \int_0^R r^2 (U^2 + V^2) dr . \quad (2.20)$$

It is now easy to compute various transport equations for the energy M

$$\partial_R M(R, t) = 4\pi R^2 \rho = \pi R^2 (U^2 + V^2) \quad (2.21)$$

$$\partial_t M(R, t) = -4\pi R^2 J = \pi R^2 (U^2 - V^2) \quad (2.22)$$

$$(\partial_R + \partial_t) M(R, t) = 2\pi R^2 U^2 \quad (2.23)$$

$$(\partial_t - \partial_R) M(R, t) = -2\pi R^2 V^2 . \quad (2.24)$$

It is clear from Eqs.(2.23) and (2.24) that V^2 and U^2 can be interpreted as the energy fluxes in the outgoing future and ingoing future null directions respectively.

III. SPHERICALLY SYMMETRIC MASSLESS SCALAR FIELDS IN SCHWARZSCHILD SPACETIME

Let us now consider a spherically symmetric massless scalar field minimally coupled to the Schwarzschild spacetime with the standard external metric

$$ds^2 = - \left(1 - \frac{2m_0}{R} \right) dt^2 + \left(1 - \frac{2m_0}{R} \right)^{-1} dR^2 + R^2 d\Omega^2 , \quad (3.1)$$

where m_0 is a positive constant, the Schwarzschild mass. While there is no explicit solution akin to Eq.(2.2), much of the analysis of Section 2 carries over. Define a ‘radiation amplitude’ $h(s, t)$, $s \in (-\infty, \infty)$, as follows

$$\begin{aligned} h_+(R, t) &= h(R, t) = \frac{1}{2} \left(-\frac{1}{\gamma} \partial_0 + \partial_R \right) (R\phi) \\ h_-(R, t) &= h(-R, t) = \frac{1}{2} \left(\frac{1}{\gamma} \partial_0 + \partial_R \right) (R\phi) . \end{aligned} \quad (3.2)$$

where $\gamma = 1 - 2m_0/R$. Given $h(R)$ the field ϕ can be recovered by a simple integration

$$\hat{h} = -\frac{1}{2R} \int_R^\infty dr [h_+(r) + h_-(r)] = \frac{1}{2} \phi . \quad (3.3)$$

The scalar field equation, $\nabla_\mu \partial^\mu \phi = 0$, Eq.(2.1), can be written as a single first order equation on a ‘symmetrized’ domain $-\infty \leq R \leq \infty$,

$$(\partial_0 + \gamma \partial_R) h = (h - \hat{h}) \frac{-2m_0 R}{|R|^3} . \quad (3.4)$$

It is useful to change coordinates and introduce the Regge-Wheeler coordinate [3] as a new radial variable

$$r^* = R + 2m_0 \ln \left(\frac{R}{2m_0} - 1 \right) . \quad (3.5)$$

Using this, equation (3.4) reads

$$(\partial_0 + \partial_{r^*}) h = (h - \hat{h}) \frac{-2m_0 R}{|R|^3} . \quad (3.6)$$

From Eq.(3.5) follows that $dR/dr^* = 1 - 2m_0/R$ and this allows us to write Eq.(3.6) as

$$(\partial_0 + \partial_{r^*}) \left[\left(1 - \frac{2m_0}{R} \right) h \right] = \frac{2m_0 R}{|R|^3} \left[\left(1 - \frac{2m_0}{R} \right) \hat{h} \right] . \quad (3.7)$$

This can be solved by

$$\left(1 - \frac{2m_0}{R}\right)h(r^*, t) = h_0(r^* - t) + \int_{(r^*-t, 0)}^{(r^*, t)} \frac{2m_0 R}{|R|^3} \left[1 - \frac{2m_0}{R}\right] \hat{h} dv, \quad (3.8)$$

where the integration in Eq.(3.8) extends along the ‘outgoing’ null ray from a point on the initial slice at $(r^* - t, 0)$ to (r^*, t) . (Of course in the negative R region, where we are dealing with h_- , the integration contour follows along the physical ingoing null ray.) It is clear that \hat{h} mixes the outgoing with the ingoing modes and thus is responsible for the backscattering. The leading term in Eq.(3.8) is just the standard gravitational redshift. One gets from Eq.(3.8) at $t = 0$

$$h_0(x) = \left(1 - \frac{2m_0}{R(x)}\right) h(x, 0), \quad (3.9)$$

and ignoring the second term in Eq.(3.8) we arrive at

$$h(r^*(0) + \tau, \tau) = \left(1 - \frac{2m_0}{R(r^*(0))}\right) \left(1 - \frac{2m_0}{R(r^*(0) + \tau)}\right)^{-1} h(r^*(0), 0), \quad (3.10)$$

when τ becomes large.

As in the Minkowski space-time case the stress-energy Eq.(2.3) naturally expressess via U and V defined below

$$U = (\gamma^{\frac{1}{2}} \partial_R + \gamma^{-\frac{1}{2}} \partial_t) \phi \quad (3.11)$$

$$V = (\gamma^{\frac{1}{2}} \partial_R - \gamma^{-\frac{1}{2}} \partial_t) \phi. \quad (3.12)$$

The relevant components of the stress-energy tensor read

$$\rho = -T_0^0 = \frac{1}{4}(U^2 + V^2) \quad (3.13)$$

$$J = -T_{0R} = \frac{1}{4}(V^2 - U^2) \quad (3.14)$$

$$T = T_R^R = \frac{1}{4}(U^2 + V^2). \quad (3.15)$$

The ‘mass function’ - the energy associated with a ball of radius R - is given by

$$m(R, t) = 4\pi \int_0^R r^2 \rho dr. \quad (3.16)$$

This is the analogue of the Misner-Sharp-Hawking-*et al* mass. Differentiation of Eq.(3.16) yields

$$\partial_R m(R, t) = 4\pi R^2 \rho = \pi R^2 (U^2 + V^2) \quad (3.17)$$

$$\partial_t m(R, t) = -4\pi R^2 J = \pi \gamma R^2 (U^2 - V^2). \quad (3.18)$$

The derivatives of m along the outgoing and ingoing null directions can be written, employing Eqs.(3.17) and (3.18), as

$$(\gamma \partial_R + \partial_t) m(R, t) = 2\pi \gamma R^2 U^2 \quad (3.19)$$

$$(\partial_t - \gamma \partial_R) m(R, t) = -2\pi \gamma R^2 V^2. \quad (3.20)$$

Let us comment on the derivation of Eq.(3.18), since it is not obvious and since that would help to understand why $m(R, t)$ is chosen as above, in a non-canonical way. There is a timelike Killing vector $\xi^\mu = (1, 0, 0, 0)$ which satisfies $\xi_{(\mu; \nu)}$. This implies, together with the stress-energy conservation law $T_{\nu; \mu}^\mu = 0$, $(T_\nu^\mu \xi^\nu)_{; \mu} = 0$. The vectorial divergence can be written as $(\sqrt{-g} T_\nu^\mu \xi^\nu)_{; \mu} = 0$; this leads to

$$-(\sqrt{-g} T_0^0)_{; 0} = (\sqrt{-g} T_0^a)_{; a}. \quad (3.21)$$

The integral of the left hand side of Eq.(3.21) over a sphere is clearly $\partial m / \partial t$ from Eq.(3.16). The integral of the right hand side is just a flat space total divergence which becomes a surface integral. From this Eq.(3.18) immediately follows.

IV. THE SPHERICALLY SYMMETRIC EINSTEIN - MASSLESS SCALAR FIELD SYSTEM

In this section we will study the full Einstein-scalar field system, including the backreaction that the matter exerts on the geometry. The polar gauge condition $trK = K_r^r$ is our slicing condition. This guarantees that the normal to the slices is along the lines of constant R . Its major attraction is that to a large degree it eliminates the extrinsic curvature from the field equations. This allows one to express the metric explicitly in terms of the matter-field. The great disadvantage is that one cannot cope with horizons in the polar gauge, thus the latter is not suitable for the descriptions of late stages of the collapse but it is useful in the exterior zone that we wish to investigate. The aforementioned choice of gauge is equivalent to choosing a diagonal line element

$$ds^2 = -\beta(R, t)\gamma(R, t)dt^2 + \frac{\beta(R, t)}{\gamma(R, t)}dR^2 + R^2(r, t)d\Omega^2, \quad (4.1)$$

where t is a time coordinate, R is a radial coordinate that coincides with the areal radius and $d\Omega^2 = d\theta^2 + \sin^2\theta d\phi^2$ is the line element on the unit sphere, $0 \leq \phi < 2\pi$ and $0 \leq \theta \leq \pi$. At spatial infinity (of an asymptotically flat spacetime) the metric coefficient g_{RR} tends to $+1$ and g_{tt} tends to -1 . Thus β and γ go to $+1$ at infinity. We adopt the standard convention that Greek letters range from 0 to 3 for spacetime objects while Latin indices range from 1 to 3 for spatial objects. The Einstein equations $G_{\mu\nu} = R_{\mu\nu} - g_{\mu\nu}R/2 = 8\pi T_{\mu\nu}$ can be written as a 1+3 system of initial constraints and evolution equations [2]. Let Σ_t be a foliation of the spacetime by Cauchy hypersurfaces, with g_{ij} the intrinsic metric and K_{ij} the extrinsic curvature. In the convention of Wald [2], $2NK_{ij} = +\partial_t g_{ij}$ and $trK = g^{ij}K_{ij}$.

As before, the scalar field is massless and spherically symmetric, with the stress-energy given by Eq.(2.3). The matter energy density is $\rho = -T_0^0$ and the matter current density is $J = -T_{0R}/\beta$. As above, we define a ‘radiation amplitude’ $h(s)$, $s \in (-\infty, \infty)$, as follows

$$h_+(R, t) = h(R, t) = \frac{1}{2}\left(-\frac{1}{\gamma}\partial_0 + \partial_R\right)(R\phi) \quad (4.2)$$

$$h_-(R, t) = h(-R, t) = \frac{1}{2}\left(\frac{1}{\gamma}\partial_0 + \partial_R\right)(R\phi). \quad (4.3)$$

One can show [5] that

$$\beta(R) = e^{-8\pi\left(\int_R^\infty + \int_{-\infty}^{-R}\right)\frac{dr}{r}(h-\hat{h})^2}, \quad (4.4)$$

where

$$\hat{h} = -\frac{1}{2R}\int_R^\infty dr[h_+(r) + h_-(r)] = \frac{1}{2}\phi. \quad (4.5)$$

γ can be expressed in the following useful form [5]

$$\gamma(R) = \frac{1}{R}\int_0^R \beta dr. \quad (4.6)$$

In spherically symmetric gravity one knows that the gravitational field is kinematical, any real dynamics is in the matter field. Therefore the metric can be expressed in terms of the matter. In the polar gauge this can be done explicitly (see Eqs. (4.4 - 4.6)).

The scalar field equation $\nabla_\mu \partial^\mu \phi = 0$ can be written as a single first order equation on a ‘symmetrized’ domain $-\infty \leq R \leq \infty$,

$$(\partial_0 + \gamma\partial_R)h = (h - \hat{h})\frac{\gamma - \beta}{R}. \quad (4.7)$$

This equation, together with definitions of h, \hat{h}, β , and γ , encodes the all information carried by the Einstein equations coupled to the scalar field. Notice that $\int_{-\infty}^\infty dr h(r) = \int_0^\infty dr [h(r) + h(-r)] = \int_0^\infty dr \partial_r \tilde{\phi} = 0$, where $\tilde{\phi} = R\phi$; therefore initial data, h_0 , of compact support must satisfy the condition

$$\int_{-\infty}^\infty dr h_0 = 0. \quad (4.8)$$

It has been shown, using relations between metric functions and their symmetry properties, that if (4.8) holds true then $\int_{-\infty}^{\infty} dr h(r, t_0) = 0$ in the existence interval of a solution. The local existence of a Cauchy solution for the above system and a global existence in an external region bounded from the interior by a null cone have also been shown ([4], [5]).

An alternative representation of γ that will be useful is

$$\gamma(R) = \left(1 - \frac{2m_0}{|R|} + \frac{2m_{ext}(R)}{R}\right)\beta(R) \quad (4.9)$$

where m_0 is the asymptotic mass and m_{ext} is a contribution to the asymptotic mass coming from the exterior of a sphere of a radius $|R|$,

$$m_{ext}(R) = 4\pi \int_{|R|}^{\infty} \frac{\gamma}{\beta} \left([h(r) - \hat{h}]^2 + [h(-r) - \hat{h}]^2 \right) dr . \quad (4.10)$$

Paralleling Eq.(3.19) we can write

$$(\partial_0 + \gamma\partial_R)m_{ext}(R) = -8\pi\gamma^2(h_- - \hat{h})^2 \quad (4.11)$$

$$(\partial_0 - \gamma\partial_R)m_{ext}(R) = 8\pi\gamma^2(h_+ - \hat{h})^2 \quad (4.12)$$

Let us stress that many of the equations written down in this section take on a quite special form in the polar gauge. In particular, the object defined in Eq.(4.10) is the Hawking mass (or mass function) which in a general gauge depends on the matter current as well as on the energy-density. In the polar gauge it simplifies, since the two null expansions are equal and the term which depends on the current drops out. Let us point out again that $h(R)$, $R > 0$, represents outgoing radiation while $h(-|R|)$ is an ingoing scalar wave.

We can substitute Eq.(4.9) into Eq.(4.7) and rewrite the scalar field equation as

$$(\partial_0 + \gamma\partial_R)h = (h - \hat{h})\frac{-2m(R)R\beta}{|R|^3} , \quad (4.13)$$

where $m(R) = m_0 - m_{ext}(R)$ is the Hawking mass at a radius R . This is similar to Eq.(3.7) but now backreaction is taken into account. Therefore our interpretation of Eq.(3.7) as giving a ‘red-shift’ due to the h term on the right-hand-side (determined by the local mass function, $m(R)$, rather than the Schwarzschild mass, m_0) and a ‘backscattering’ due to the \hat{h} term should remain valid in some appropriate limit.

In going from Eq.(3.6) to Eq.(3.7) we found what was essentially an integration function, $(1 - 2m_0/R)$, which allowed us eliminate the term in h on the right-hand-side of Eq.(3.6). It turns out that this trick can be repeated with Eq.(4.13).

Let us define

$$\ln \left[1 - \frac{2\tilde{m}(R)}{R} \right] = - \int_R^{\infty} \frac{2m(r)dr}{r^2(1 - 2m(r)/r)} , \quad (4.14)$$

where the integral is taken along an outgoing null ray. From Eq.(4.12) follows that the mass function monotonically increases along an outgoing null ray and also that $m(R) \rightarrow m_{BR_0}$ (the ‘local Bondi mass’ that can be assigned to a future null cone starting from R_0). Consider a null ray which starts at R_0 ; then $m(R_0) \leq m(r) \leq m_{BR_0}$. This immediately gives

$$\frac{2m(R_0)}{r^2(1 - 2m(R_0)/r)} \leq \frac{2m(r)}{r^2(1 - 2m(r)/r)} \leq \frac{2m_{BR_0}}{r^2(1 - 2m_{BR_0}/r)} . \quad (4.15)$$

Integration of this equation along the null cone yields

$$1 - \frac{2m(R_0)}{R} \geq 1 - \frac{2\tilde{m}(R)}{R} \geq 1 - \frac{2m_{BR_0}}{R} . \quad (4.16)$$

Since $m(R_0) \rightarrow m_{BR_0}$ as $R_0 \rightarrow \infty$ we conclude that $\tilde{m}(R) \rightarrow m_{BR_0}$. $m(R)$ is positive along an outgoing null cone hence it is clear that $1 - 2\tilde{m}(R)/R$, which is going to be our redshift factor, is monotonically increasing. Note that there is no guarantee that $1 - 2m(R)/R$ is monotonic.

Using Eq(4.14) and Eq.(4.9), it is easy to rewrite Eq.(4.13) as

$$(\partial_0 + \gamma \partial_R) \left(1 - \frac{2\tilde{m}(R)}{R}\right) h = \hat{h} \left(1 - \frac{2\tilde{m}(R)}{R}\right) \frac{2m(R)R\beta}{|R|^3}. \quad (4.17)$$

or as a pair of equations on the half-line, $R \geq 0$,

$$(\partial_0 + \gamma \partial_R) \left(1 - \frac{2\tilde{m}(R)}{R}\right) h_+ = \hat{h} \left(1 - \frac{2\tilde{m}(R)}{R}\right) \frac{2m(R)\beta}{R^2} \quad (4.18)$$

$$(\partial_0 - \gamma \partial_R) \left(1 - \frac{2\tilde{m}(R)}{R}\right) h_- = -\hat{h} \left(1 - \frac{2\tilde{m}(R)}{R}\right) \frac{2m(R)\beta}{R^2}; \quad (4.19)$$

similar to equation (3.7). Reasoning as in Section III leads to a clean separation between redshift and backscattering.

V. WEAK FIELD - REDSHIFT AND BACKSCATTER

We can define the whole problem in the exterior domain, independent of whatever is happening in the interior. Already \hat{h} , Eq.(4.5), is defined in a proper form. Given (4.8), \hat{h} can be written as

$$\hat{h} = -\frac{1}{2R} \left[\int_{-\infty}^{-R} + \int_{+R}^{\infty} \right] dr h(r) = \frac{1}{2} \phi. \quad (5.1)$$

It is clear, from Eq.(4.4), that $\beta(R)$ is only dependent on external quantities. The calculation of $\gamma(R)$, requires the use Eq.(4.6), together with the fact that, at infinity, γ behaves like $1 - 2m_0/R$ while β goes quickly to 1. This allows us to write

$$\gamma(R) = 1 - \frac{2m_0}{R} + \frac{1}{R} \int_R^{\infty} [1 - \beta(r)] dr; \quad (5.2)$$

thus there are two equivalent expressions for $m_{ext}(R)$, Eq.(4.10) and

$$m_{ext}(R) = \frac{1}{2} \int_R^{\infty} [1 - \beta(r)] dr. \quad (5.3)$$

The form of Eq.(4.10) inspires one to write Eq.(4.4) as

$$\beta(R) = e^{-8\pi \left(\int_R^{\infty} + \int_{-R}^{-\infty} \right) \frac{\beta}{\gamma r} (h - \hat{h})^2 dr}. \quad (5.4)$$

Eq.(4.9) gives the inequality

$$\frac{\beta}{\gamma r} = \frac{1}{r - 2m(r)} \leq \frac{1}{r - 2m_0}. \quad (5.5)$$

The factor $\beta/\gamma r$ can be taken out of the integral in Eq.(5.4) and replaced with its value at $r = R$. The remainder is then essentially Eq.(4.10). Select an ϵ and an R_A such that simultaneously $m(R_A) \approx m_0$, $m_{ext}(R_A)/m_0 < \epsilon$ and $R_A > (1 + \epsilon)2m_0$. If $R > R_A$ then

$$1 \geq \beta(R) \geq \beta(R_A) \geq e^{-2 \frac{m_{ext}(R_A)}{R_A - 2m_0}} \geq e^{-\frac{m_{ext}(R_A)}{\epsilon m_0}} \simeq 1 - O(m_{ext}/\epsilon m_0). \quad (5.6)$$

In the same vein, using Eq.(4.9) we get

$$\gamma(R) \simeq 1 - \frac{2m_0}{|R|} + O(m_{ext}/\epsilon m_0). \quad (5.7)$$

Thus ϵ and R_A should be chosen in such a way that $m_{ext}/\epsilon m_0 \ll 1$. The last two expressions imply that the condition that backreaction is negligible is not that $m_{ext} \ll m_0$ but rather $m_{ext} \ll \epsilon m_0$; in regions close to a horizon even if $\epsilon \ll 1$, a small cloud of matter can strongly influence the geometry. Estimates (5.6) and (5.7) hold, for instance, for $R_A \geq 2m_0(1 + \sqrt{m_{ext}/m_0})$. In this case

$$1 \geq \beta(R) \geq \beta(R_A) \simeq 1 - O(\sqrt{m_{ext}/m_0}), \quad (5.8)$$

and

$$\gamma(R) \simeq 1 - \frac{2m_0}{|R|} + O(\sqrt{m_{ext}/m_0}). \quad (5.9)$$

In what follows our interest is focused on the region $R > 3m_0$, since only in that region of spacetime we get sensible analytic estimates. This is equivalent to the choice $\epsilon \geq 1/2$.

For $R > 3m_0$ the scalar wave equation Eq.(4.17) can be approximated as

$$(\partial_0 + \gamma\partial_R)(1 - \frac{2m_0}{R})h = \hat{h}(1 - \frac{2m_0}{R})\frac{m_0R}{|R|^3}; \quad (5.10)$$

from the preceding analysis it follows that the error terms are of order m_{ext}/m_0 . Thus, in the limit of $m_{ext}/m_0 \ll 1$ we recover the Schwarzschild background scalar field equation, Eq.(3.5), with a solution Eq.(3.8) consisting both of the redshift and the backscattering terms.

It turns out that m_{ext} can be used in another role. It is essentially the integral of the square of the first derivative of ϕ and so one can use it to bound the pointwise value of $\phi = 2\hat{h}$. One can show, improving a coefficient in an inequality of [5], that

$$|\hat{h}| \leq \frac{\sqrt{m_{ext}}}{R^{1/2}\sqrt{8\pi(1 - \frac{2m_0}{R})}}. \quad (5.11)$$

(An estimate similar to this, but written with the total Bondi mass m_0 in place of m_{ext} , appears in [6].) Thus the solution of Eq.(5.10) can be estimated by solutions of following equations

$$(\partial_0 + \partial_{r^*})\left((1 - \frac{2m_0}{R})h\right) = -\frac{2m_0(1 - \frac{2m_0}{R})\sqrt{m_{ext}}}{R^{5/2}\sqrt{8\pi(1 - \frac{2m_0}{R})}}, \quad (5.12)$$

$$(\partial_0 + \partial_{r^*})\left((1 - \frac{2m_0}{R})h\right) = +\frac{2m_0(1 - \frac{2m_0}{R})\sqrt{m_{ext}}}{R^{5/2}\sqrt{8\pi(1 - \frac{2m_0}{R})}}, \quad (5.13)$$

where the minus and plus signs gives a bound from below and above, respectively. The solution of Eq. (5.12) the same as of Eq.(3.8)

$$\left(1 - \frac{2m_0}{R(r)}\right)h(r^*, t) = h_0(r^* - t) + \sqrt{\frac{m_{ext}}{8\pi}}2m_0 \int_{(r-t,0)}^{(r,t)} \left(1 - \frac{2m_0}{R}\right) dv \frac{1}{R^2\sqrt{R-2m_0}} \quad (5.14)$$

and equation (5.13) is solved by

$$\left(1 - \frac{2m_0}{R(r)}\right)h(r^*, t) = h_0(r^* - t) - \sqrt{\frac{m_{ext}}{8\pi}}2m_0 \int_{(r-t,0)}^{(r,t)} \left(1 - \frac{2m_0}{R}\right) dv \frac{1}{R^2\sqrt{R-2m_0}} \quad (5.15)$$

Notice that that the dv in the integrals in Eqs.(5.14) and (5.15) is essentially dr^* , the Regge-Wheeler coordinate introduced in Eq.(3.6) with $dR/dr^* = 1 - 2m_0/R$. Therefore the integral can be written in closed form as

$$\sqrt{\frac{m_{ext}}{\pi}}m_0 \int \frac{dR}{R^2\sqrt{(R-2m_0)}} = \sqrt{\frac{m_{ext}}{2\pi}}m_0 \left[\frac{\sqrt{R-2m_0}}{2m_0R} + \frac{1}{2m_0\sqrt{2m_0}} \arctan \sqrt{\frac{R-2m_0}{2m_0}} \right] \quad (5.16)$$

$$= \sqrt{\frac{m_{ext}}{16\pi m_0}} \left[\sqrt{\frac{2m_0}{R}} \left(1 - \frac{2m_0}{R}\right) + \arctan \sqrt{\frac{R-2m_0}{2m_0}} \right]. \quad (5.17)$$

From Eq.(5.17) not only can we see that the redshift term in the solution (Eq.(5.14) or (5.15)) is correct up to terms of order m_{ext}/m_0 , we can also see that the total backscattering is bounded by a term of order $\sqrt{m_{ext}/m_0}$. Thus in the limit where m_{ext}/m_0 is small, the standard gravitational redshift represented by Eq.(3.10) is recovered and this is valid along an outgoing null ray to an accuracy of $O(\sqrt{m_{ext}/m_0})$. Let us stress that this holds in a strong gravitational field. We need not assume $R \gg m_0$, but only $R > 3m_0$.

The estimate of the backscattering, Eq.(5.17), is amazingly regular. It equals 0 when $R = 2m_0$, remains always positive, monotonically increases and has a maximum value of $\sqrt{\pi m_{ext}/64m_0}$ when $R \rightarrow \infty$. It rises quite rapidly to about 1/3 of its final value when $R = 3m_0$ and about 0.8 of its final value when $R = 4m_0$. This means that the backscattering is only important deep in the potential well and its contribution rapidly diminishes as one considers radiation which is starting off further and further out. The redshift factor, $\gamma = 1 - 2m_0/R$ is much more severe and the energy flux (or the magnitude of h) is severely diminished if one starts close to the horizon.

More detailed information about the nature and magnitude of the backscattering term will be given in the next section.

VI. BACKSCATTERING

Let us assume initial data which (at $t = 0$) represent a pure outgoing wave, i. e., $h_- \equiv 0$ or (equivalently) $h(R, 0) = 0$ for $R < 0$. Let us take a point to the future (R_1, T_1) , outside any horizon, $R_1 > 2m_0$; $R_1 \geq 3m_0$ would even be better in order to guarantee that backreaction is absent. Consider the ingoing future radial null ray which passes through (R_1, T_1) . This will start from the initial hypersurface at some point $(R_0, 0)$ with $R_0 > R_1$. Along this null ray R monotonically decreases while m_{ext} monotonically increases. Eq.(5.17) implies

$$\left(1 - \frac{2m_0}{R_1}\right) |h_-(R_1, T_1)| \leq \sqrt{\frac{m_{ext}}{16\pi m_0}} \left[\sqrt{\frac{2m_0}{R_0} \left(1 - \frac{2m_0}{R_0}\right)} + \arctan \sqrt{\frac{R_0 - 2m_0}{2m_0}} \right. \\ \left. - \sqrt{\frac{2m_0}{R_1} \left(1 - \frac{2m_0}{R_1}\right)} - \arctan \sqrt{\frac{R_1 - 2m_0}{2m_0}} \right], \quad (6.1)$$

where m_{ext} is $m_{ext}(R_1, T_1)$. This expression is valid to an accuracy of $O(m_{ext}/m_0)$ and has an upper bound of $\sqrt{\pi m_{ext}/64m_0}$ which is achieved when T_1 is large and $R_1 \approx 2m_0$. It reduces rapidly as R_1 increases, it is down to 1/5 of this value when $R_1 = 4m_0$ as already discussed in Section 5. Far out along an outgoing null cone, where $R_1 \approx T_1 \gg m_0$ and where $R_0 \approx 2R_1$, it goes to zero like $R_1^{-3/2}$. In this regime the analysis of Sections 2 and 3 would hold. Therefore one could expect to approximate \hat{h} by $g(R-t)/2R$. Further, approximating $g(R-t)$ by a step function of finite width and substituting this into Eq.(3.8), one expects h_- to fall off like R_1^{-3} .

Take an outgoing null ray through the point $(R_1, 0)$ which forms the inner boundary of the outgoing wave. We estimate h_- along this null ray, using Eq.(6.1), and \hat{h} . The integration of Eq.(4.12) along this null ray yields an estimate of the total energy flux across this surface in the inward direction. This will be the total energy loss from the outgoing wave due to backscattering.

To get explicit estimates, let us further approximate the integral in Eq.(5.16): R monotonically decreases along the ingoing lightray, so one can just replace the $\sqrt{1 - 2m_0/R}$ by $\sqrt{1 - 2m_0/R_1}$. This yields

$$\sqrt{\frac{m_{ext}}{2\pi}} m_0 \int_{R_1}^{R_0} \frac{dR}{R^2 \sqrt{R - 2m_0}} \leq \sqrt{\frac{m_{ext} R_1}{2\pi(R_1 - 2m_0)}} m_0 \int dR R^{-5/2} \quad (6.2)$$

$$= \sqrt{\frac{m_{ext} R_1}{2\pi(R_1 - 2m_0)}} m_0 \left[\frac{2}{3R_1^{3/2}} - \frac{2}{3R_0^{3/2}} \right] \quad (6.3)$$

$$\leq \sqrt{\frac{m_{ext} R_1}{2\pi(R_1 - 2m_0)}} m_0 \left(\frac{2}{3}\right) R_1^{-3/2}. \quad (6.4)$$

Thus we arrive at

$$|\gamma h_-(R)| \leq \frac{2}{3} \sqrt{\frac{m_{ext}}{2\pi m_0}} \left[\frac{m_0^{3/2}}{R \sqrt{R - 2m_0}} \right]. \quad (6.5)$$

Knowing h_- , one can use its definition, Eq.(4.3), to compute $R\phi$ and hence ϕ and \hat{h} . Eq.(4.3) yields the inequality

$$(\partial_0 + \partial_{r^*})(R\hat{h}) = \gamma h_- \leq \frac{2}{3} \sqrt{\frac{m_{ext}}{2\pi m_0}} \left[\frac{m_0^{3/2}}{R(R - 2m_0)^{1/2}} \right]; \quad (6.6)$$

a similar inequality with minus sign gives a lower bound.

These can be solved in the standard way to give (remembering to change from dr^* to dR)

$$|R\hat{h}(R, t)| \leq |R\hat{h}(R_2, 0)| + \frac{2}{3} \sqrt{\frac{m_{ext}}{2\pi m_0}} m_0^{3/2} \int \frac{dR}{(R - 2m_0)^{3/2}}, \quad (6.7)$$

where we assume that the outgoing null cone starts at $(R_2, 0)$. The integration gives

$$|R\hat{h}(R, t)| \leq |R\hat{h}(R_2, 0)| + \frac{4}{3} \sqrt{\frac{m_{ext}}{2\pi m_0}} \frac{m_0^{3/2}}{(R_2 - 2m_0)^{1/2}} - \frac{4}{3} \sqrt{\frac{m_{ext}}{2\pi m_0}} \frac{m_0^{3/2}}{(R - 2m_0)^{1/2}}. \quad (6.8)$$

Now let us choose this outgoing null ray inside the outgoing burst of radiation; there is neither an ingoing nor an outgoing field, i.e., $h_+ = h_- \equiv 0$. This does not imply $\phi/2 = \hat{h} \equiv 0$. Rather it only implies $R\phi = C$, with C a constant. This looks like the static field of a point charge. If there is a regular center, this would be excluded, but in the case of a black hole, or if there is some sort of complicated interior this cannot *a priori* be ruled out. On the other hand such a ‘static’ field has energy density and this will cause the mass function to vary along the lightcones. We are not interested in such variation focusing only in evaluating the change in the mass function due to backscattering. Therefore we make the extra assumption that $\phi(R_2, 0) = 0$. This means that the first term in Eq.(6.8) vanishes.

It is clear that the last term in Eq.(6.8) is strictly larger than $|h_-|$ as given by Eq.(6.5) if $R > 4m_0$ (i. e., when all radiation is placed outside $4m_0$). Thus

$$|\hat{h} - h_-| \leq |\hat{h}| + |h_-| \leq \frac{4}{3} \sqrt{\frac{m_{ext}}{2\pi m_0}} \frac{m_0^{3/2} R_2}{R(R_2 - 2m_0)^{1/2}}. \quad (6.9)$$

The integration of Eq.(4.11) from R_A to ∞ gives a bound for the total change in m_{ext} ,

$$\Delta m_{ext} \leq m_{ext} \frac{16}{9} \left(\frac{2m_0}{R_2} \right)^2 \left(\frac{1 - m_0/R_2}{1 - 2m_0/R_2} \right). \quad (6.10)$$

This expression demonstrates how sensitive the amount of backscattering is to the location of the innermost null cone. This estimate becomes meaningless if $R_2 \approx 3.5m_0$ because $\Delta m_{ext} \geq m_{ext}$. In the case of a neutron star, where $2m_0/R \leq 0.1$ (on the surface of the star) we have an upper bound for the backscattered energy of 2% of m_{ext} .

The above estimation can be significantly refined when initially outgoing pulses are far enough from the apparent horizon. The basic point uses the following argument. Take an outgoing null ray which starts at a point $(R_2, 0)$ and which goes through (R_1, T_1) . Consider also the incoming null ray which starts at $(R_0, 0)$. These have corresponding tortoise coordinates $r^*(2), r^*(1), r^*(0)$ as defined by Eq.(3.5). They satisfy

$$r^*(0) - \tau(1) = r^*(1) = r^*(2) + \tau(1). \quad (6.11)$$

While it is NOT true that $R_0 < 2R_1$ in general, it is *almost* true and it is certainly true, for instance when $R_2 \geq 12m_0$. In going from Eq.(6.3) to Eq.(6.4) one can legitimately replace R_0 by $2R_1$. That allows one to get in (6.5) the additional factor $\alpha \equiv \frac{\sqrt{2}-1/2}{\sqrt{2}}$. (6.5) reads

$$|R\hat{h}(R, t)| \leq |R\hat{h}(R_2, 0)| + 2 \frac{2\sqrt{2}-1}{3\sqrt{2}} \sqrt{\frac{m_{ext}}{\pi m_0}} m_0^{3/2} \int \frac{dR}{(R - 2m_0)^{3/2}}, \quad (6.12)$$

assuming that the outgoing null cone starts at $(R_2, 0)$. While it is possible to solve this integral explicitly, an interesting approximation can be found by extracting the $1 - 2m_0/R$ and replacing it with $1 - 2m_0/R_2$ to get

$$|R\hat{h}(R, t)| \leq |R\hat{h}(R_2, 0)| + \frac{8\sqrt{2}-4}{3\sqrt{2}} \sqrt{\frac{m_{ext}}{2\pi m_0}} \frac{m_0^{3/2}}{(1 - 2m_0/R_2)^{3/2}} \left[\frac{1}{\sqrt{R_2}} - \frac{1}{\sqrt{R}} \right]. \quad (6.13)$$

Now the second term is more than twice as large as the estimate for $|h_-|$. Thus we may conclude that

$$|\hat{h} - h_-| \leq \frac{8\sqrt{2}-4}{3\sqrt{2}} \sqrt{\frac{m_{ext}}{2\pi m_0}} \frac{m_0^{3/2}}{(1 - 2m_0/R_2)^{3/2}} \left[\frac{1}{R\sqrt{R_2}} - \frac{1}{2R^{3/2}} \right]. \quad (6.14)$$

Therefore, the total change in m_{ext} can be obtained by inserting the above into Eq.(4.11) and integration from R_2 to ∞ , which yields

$$\Delta m_{ext} \leq \frac{\alpha^2 16}{9} \left(\frac{2m_0}{R_2} \right)^2 \frac{(1 - m_0/R_2)}{1 - 2m_0/R_2} m_{ext}. \quad (6.15)$$

That estimate is better than the former one by the factor of $\alpha^2 \simeq 0.4$. Applying that to case of neutron stars, when the conditions assumed above hold true, we can get that the maximal amount of (possibly) backscattered radiation does not exceed 1 percent.

The initially outgoing field, h_+ , generates a weaker ingoing field, h_- , which enters the ‘no-radiation’ zone behind the wavefront. This, in turn, scatters again off the gravitational field to generate a new outgoing field, which turns up at null infinity at a later time, after the first burst of outgoing radiation has gone. This is called the ‘tail’ term. Eq.(6.9) gives an estimate for \hat{h} in the ‘no-radiation’ zone. Let us substitute this back into the scalar wave equation, say Eq.(5.10), and estimate the second order h_+ along the outgoing null ray. We get

$$|\gamma h_+(R, t)| \leq \frac{8}{3} \sqrt{\frac{m_{ext}}{2\pi m_0}} \frac{m_0^{5/2}}{\sqrt{R_2 - 2m_0}} \int_{R_2}^R \left[\frac{1}{R^3} - \frac{\sqrt{R_2 - 2m_0}}{R^3 \sqrt{R - 2m_0}} \right] dR. \quad (6.16)$$

Throwing away the second term in Eq.(6.16) and integrating Eq.(6.16) gives

$$|\gamma h_+(R, t)| \leq \frac{8}{3} \sqrt{\frac{m_{ext}}{2\pi m_0}} \frac{m_0^{5/2}}{\sqrt{1 - 2m_0/R_2}} \left[\frac{1}{3R_2^{5/2}} - \frac{1}{3R^2 \sqrt{R_2}} \right] dR. \quad (6.17)$$

In the limit as $R \rightarrow \infty$ along the null cone we get

$$|h_+(\infty, \infty)| \leq \frac{8}{9} \sqrt{\frac{m_{ext}}{2\pi m_0}} \frac{(m_0/R_2)^{5/2}}{\sqrt{1 - 2m_0/R_2}}. \quad (6.18)$$

That should be compared with the leading term in (5.14), h_0 ; resorting to the definition of the external mass m_{ext} , we arrive to the conclusion that the tail term is smaller than the leading term by a factor $(m_0/R_0)^2$.

VII. NUMERICAL RESULTS.

In order to estimate quantitatively the effect of backscattering we solve numerically Eqs.(4.18, 4.19 and 4.5) neglecting backreaction (i.e. dropping terms of order m_{ext}/m_0) and calculate $m_{ext}(R)$ using Eq.(4.10).

The basic evolution Eqs.(4.18, 4.19) are solved with a help of modified MacCormack predictor-corrector scheme [9], [10]. An integral defining \hat{h} in Eq.(4.5) is calculated by means of the extended trapezoidal rule. The whole procedure is second-order accurate in both space and time.

We use the following form of initial data:

$$h_+(R) = A_0(R - R_0) \exp(-20(R - R_0)^2/s^2) \quad (7.1)$$

$$h_-(R) = 0. \quad (7.2)$$

where A_0 – amplitude, R_0 – position of peak center, s – the measure of its width. This data fulfills the constraint of Eq.(4.8).

A sample of results is summarized in Figures 1 and 2 where the evolution of h_+ and \hat{h} functions is shown. Notice the effects of the redshift and widening of the h_+ profile caused by the light-cone structure in the vicinity of the horizon.

As a quantitative measure of backscattering we take the mass flux ratio:

$$r_m(T) = \frac{(m_{ext}(R, T) - m_{ext}(R_i, 0))}{m_{ext}(R_i, 0)}. \quad (7.3)$$

where $(R_i, 0)$ and (R, T) are connected by an outgoing future radial null ray.

Backscattering is noticeable close to the horizon in the regions where the \hat{h} function is significant. We do not observe a significant effect outside an impulse – the observed flux through the inner boundary of a signal defined as a radius which contains initially 90 % of m_{ext} is less than 1 % (Figure 3, long dashed line). We do observe, however, a significant effect due to backscattering deep inside a region filled with radiation. The total leakage of mass is of the order of 10 % for $R_i = R_0$, where R_0 is the position of the peak center in the initial configuration ansatz for a configuration starting from $R_0 = 1.5R_{hor} = 3m_0$ (see Figure 4, solid line). This effect decreases with the distance from the horizon, for a similar configuration starting from $R_0 = 3R_{hor} = 6m_0$ the effect is less than 2% (see Figure 3, short dashed line).

From this we can conclude that backscattering deforms signals. Thus, assuming that a source mechanism for the radiation is known, we should in principle be able to detect backscattering in pulses or bursts of radiation coming to us from compact objects like massive neutron stars or black holes.

VIII. BACKSCATTERING: ASTROPHYSICAL IMPLICATIONS?

We expect that massless spin-1 field (the photons) will behave in a very similar fashion to the massless spin zero field we have been discussing here. It is clear that two mechanisms effect the outgoing radiation. One, the redshift effect diminishes the intensity and frequency of the outgoing radiation, but the total energy in the radiation (as measured by the mass function) remains unchanged. This effect becomes larger and larger as the source approaches the horizon; the intensity is just multiplied essentially by $\gamma = 1 - 2m_0/R$.

The other effect is backscattering. The estimates that we derived in Section VI are not sharp but they are valid at least to within an order of magnitude, as the numerical results show. A quasi-stationary radiating plasma surrounding a black hole will produce radiation; some of the ingoing radiation will be reflected outwards (the black hole can act as a kind of a mirror) while some of the outgoing radiation will be reflected back. The reflection coefficients need not to be symmetric - presumably much more of the outgoing radiation will be reflected back - hence the radiation observed at infinity should be reduced below that expected when only the redshift factors are taken into account. The overall weakening of radiation in quasi-stationary systems may be of astrophysical significance in modelling activity of galactic nuclei powered by black holes, for instance a nuclei of the elliptical galaxy M87. That nuclei seems to be much less luminous than it should be, based on the standard accretion models ([7], [8]). Backreaction is certainly unable to explain the full extent of the existing discrepancy, but it can contribute to the possible explanation if the bulk of the radiation is produced at distances of a few Schwarzschild radii, when backscattering can play an important role.

Numerical results of Section VII demonstrate also another effect, namely up to 10% of the scalar field radiation emitted at $R = 3m_0$ is lost from the main impulse - even if it reaches infinity, it does so with a significant delay. More precisely, Figure 3 shows, that for an extended pulse of radiation, its 'first' half is weakened, while the other gains in intensity. Thus the shape of the pulse is deformed. That opens another possibility for detecting backscattering, namely through the investigation of short-lived signals coming from an immediate vicinity of compact bodies. One class of phenomena, X-ray bursts, are already known to result from energetic processes on a surface of neutron stars [11], so they constitute a natural object of interest, albeit in that case the backscattering is rather weak, less than 1 percent. The most interesting situation would be a merger of a neutron star and a black hole, since the effect would be then relatively strong. If gamma ray bursts [12] result in the latter type of collision, then sufficiently precise observations should reveal imprints of bacscattering in the main burst as well in the afterglow. Their definitive absence would strongly favour alternative scenarios for the formation of gamma ray bursts.

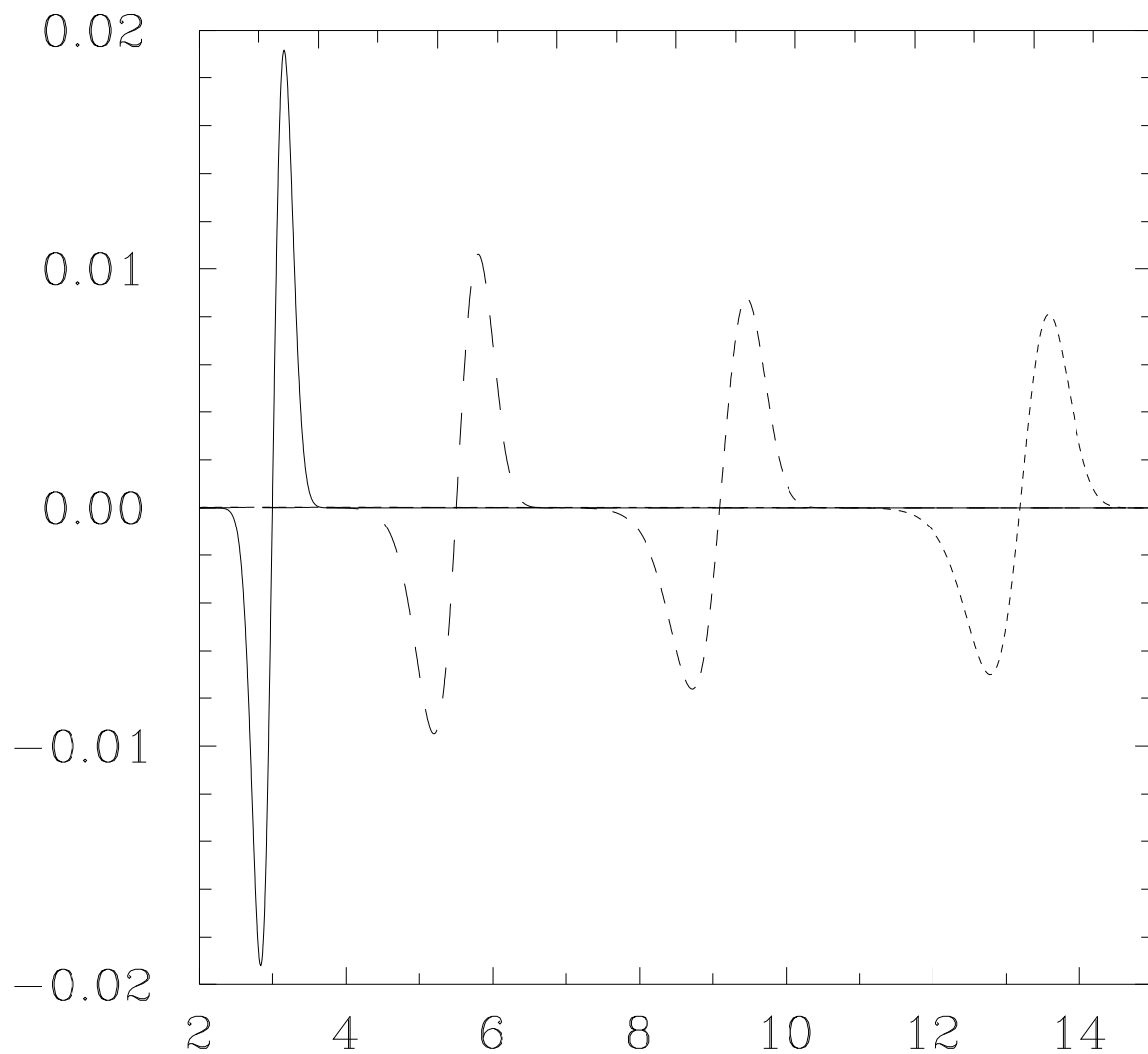


FIG. 1. An example of h_+ evolution. An initial profile defined by Eq.(7.1) with parameters $A_0 = 0.2$, $R_0 = 3$, $s = 1$, $m_0 = 1$ (solid line) and profiles corresponding to $t = 5$ (long dashed), $t = 10$ (middle dashed) and $t = 15$ (short dashed) are plotted.

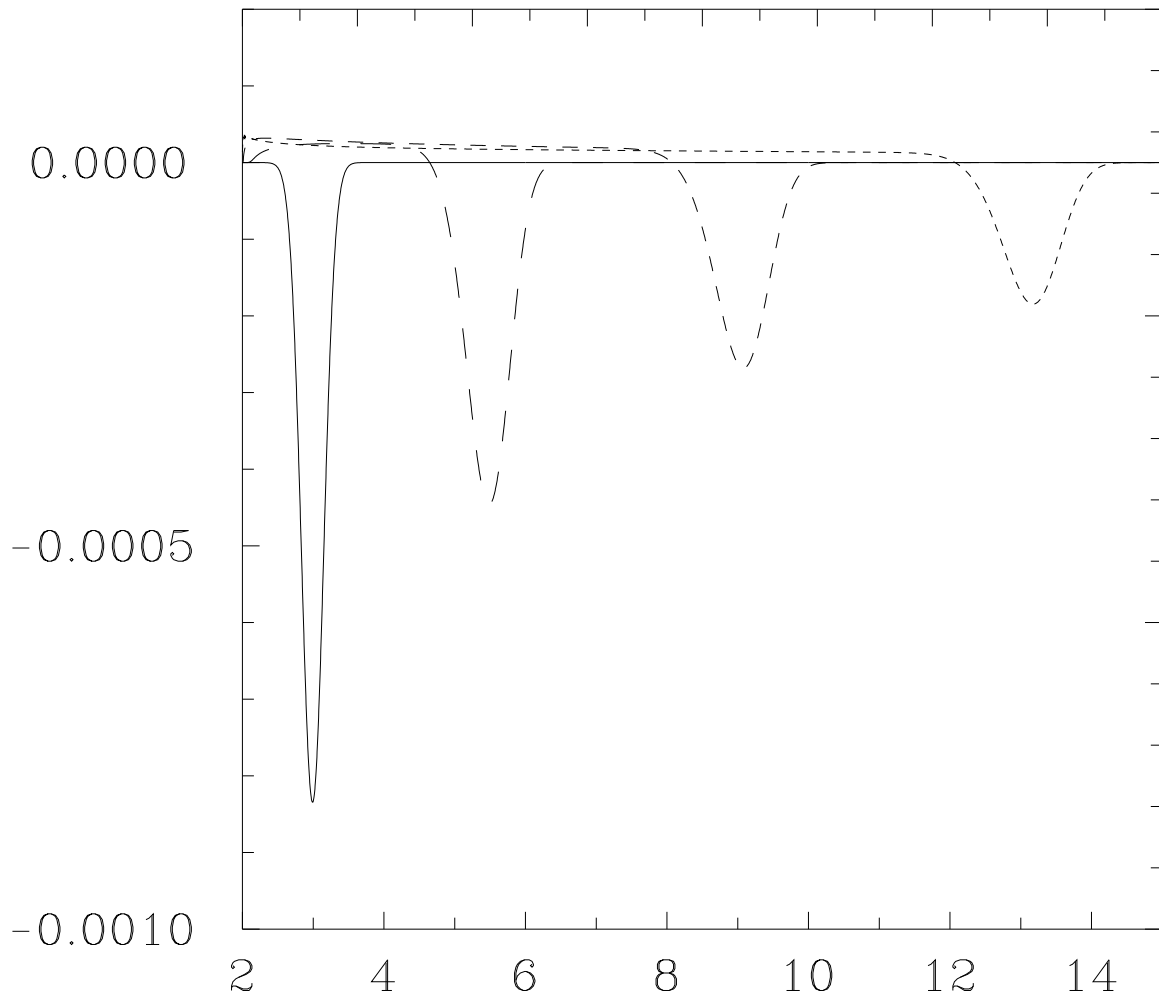


FIG. 2. An example of \hat{h} evolution. Parameters of initial configuration and time sequence as in Figure 1.

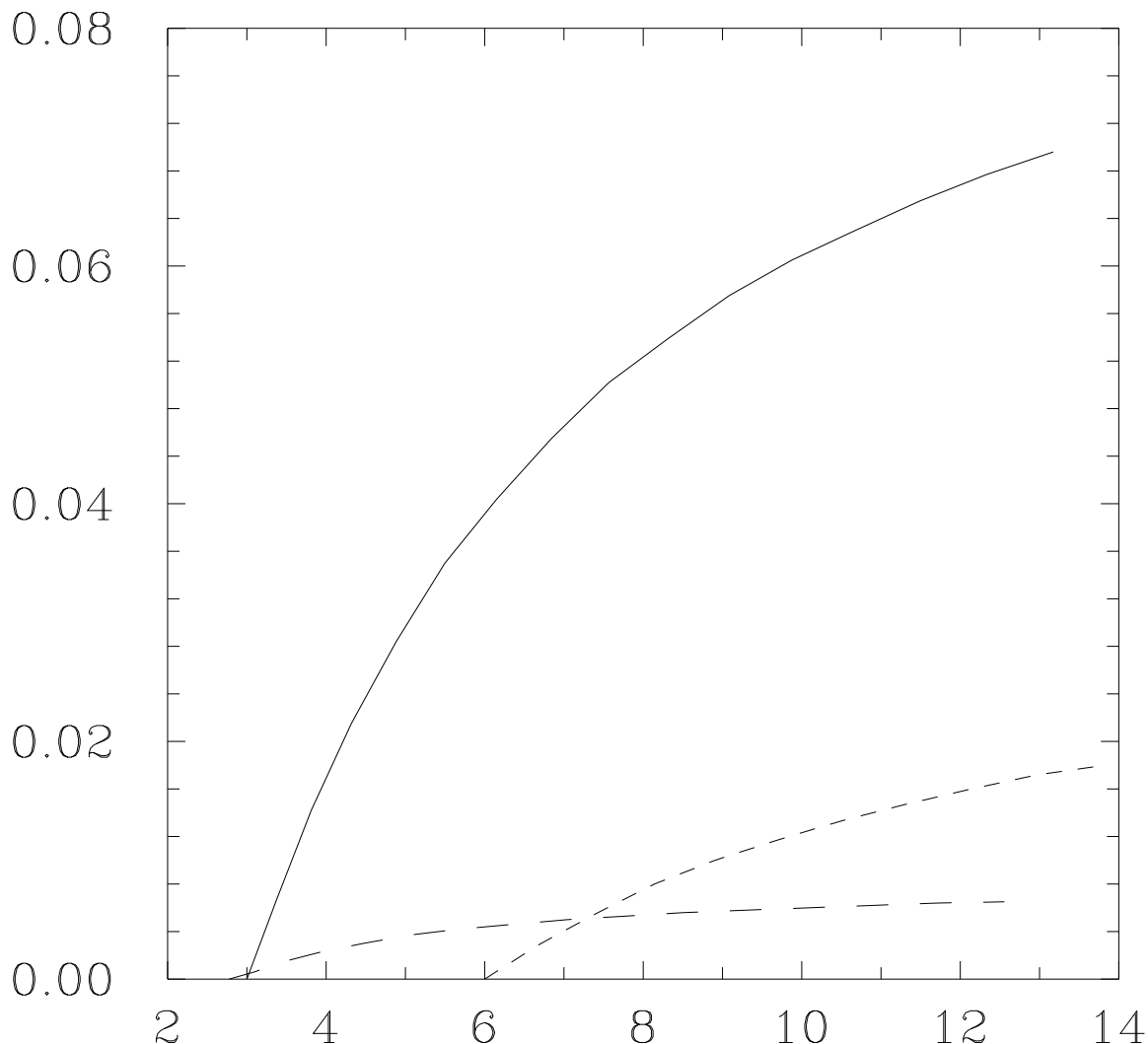


FIG. 3. Examples of leakage through null cones - mass flux ratio $r_m(T)$ through different outgoing future radial null rays as a function of position along the ray $R(T)$. The curves correspond to the following sets of parameters: solid line - $R_i = R_0 = 3, s = 1, A_0 = 0.2, m_0 = 1$; short dashed line - $R_i = R_0 = 6, s = 1, A_0 = 0.2, m_0 = 1$; long dashed line - $R_i = 2.776, s = 1, A_0 = 0.2, m_0 = 1$.

ACKNOWLEDGMENTS

This work has been partially supported by the Forbairt grant SC/96/750 and the KBN grant 2 PO3B 090 08.

-
- [1] A. Bachelot, *J. Math. Pures Appl.* **76**, 155(1997). N. Sanchez, *J. Math. Phys.* **17**, 688(1976).
 - [2] R. Wald, *General Relativity*, Chicago University Press 1984.
 - [3] C. Misner, K. Thorne, J. A. Wheeler, *Gravitation*, Freeman, San Francisco, 1973.
 - [4] E. Malec *Classical and Quantum Gravity* **13**, 1849(1996).
 - [5] E. Malec, *Journal of Mathematical Physics* **38**, 3650(1997).
 - [6] D. Christodoulou, *Commun. Math. Phys.* **106**, 487(1987).
 - [7] C. S. Reynolds et al., *The "quiescent" black hole in M87*, astro-ph/9610097.

- [8] R. Narayan and I. Yi, *Astrophysical Journal* **452**, 710(1995); Abramowicz et al., *Astrophysical Journal* **438**, L37(1995).
- [9] C. Hirsch, *Numerical computation of internal and external flows*, Vol.2 (Wiley, New York, 1990).
- [10] E. Seidel and W.M. Suen, *Phys. Rev.* **D42**, 384 (1990).
- [11] W. H. Lewin, J. von Paradijs and R. Tamm, in: *X-Ray Binaries* (Eds: G. Lewis, J. von Paradijs and E. van den Heuvel), Cambridge University Press (1995).
- [12] for a review see B. Paczyński, *Publ. astron. Soc. Pac.* **167**, 1167(1995).